

Published on

## *Wind and Structures*

Vol. **24**, No. 6 (2017) 565-578

# Numerical simulations of mountain winds in an alpine valley

Antonio Cantelli<sup>1</sup>, Paolo Monti<sup>\*2</sup>, Giovanni Leuzzi<sup>2</sup>, Giulia Valerio<sup>3</sup>  
and Marco Pilotti<sup>3</sup>

<sup>1</sup>DIMA, Università degli Studi di Roma “La Sapienza”, Via Eudossiana 18, Roma, Italy

<sup>2</sup>DICEA, Università degli Studi di Roma “La Sapienza”, Via Eudossiana 18, Roma, Italy

<sup>3</sup>DICATAM, Università di Brescia, Via Branze 43, Brescia, Italy

**Abstract.** The meteorological model WRF is used to investigate the wind circulation in Valle Camonica, Italy, an alpine valley that includes a large subalpine lake. The aim was to obtain information necessary to evaluate the wind potential of this area and, from a methodological point of view, to suggest how numerical modeling can be used to locate the most interesting spots for wind exploitation. Two simulations are carried out in order to analyze typical scenarios occurring in the valley. In the first one, the diurnal cycle of thermally-induced winds generated by heating-cooling of the mountain range encircling the valley is analyzed. The results show that the mountain slopes strongly affect the low-level winds during both daytime and nighttime, and that the correct setting of the lake temperature improves significantly the quality of the meteorological fields provided by WRF. The second simulation deals with an event of strong downslope winds caused by the passage of a cold front. Comparisons between simulated and measured wind speed, direction and air temperature are also shown.

**Keywords:** alpine valley; complex terrain; katabatic flows; lake Iseo; WRF.

## 1. Introduction

The weather in mountainous regions is influenced mainly by local atmospheric circulations (see Whiteman 2000 for a comprehensive review on this topic). Valleys and escarpments are sheltered from synoptic-wind systems, causing their micrometeorology to be strongly dependent on local thermal forcing (Fernando *et al.* 2001). The flow therein is determined mostly by the differential heating-cooling of uneven terrain (thermally-driven circulations) and its prediction presents considerable difficulties, particularly when the terrain is significantly complex, since the flow is very sensitive to details of the topography. The daytime wind is typically upslope (also known as anabatic flow), while the nighttime wind is downslope (katabatic or drainage flow). Slope flows are characterized by sustained wind speeds (generally 1-4 ms<sup>-1</sup>), and the transition between slope flows in the early morning and in the late afternoon is generally accompanied by low winds.

---

\*Corresponding author, Assistant Professor, E-mail: paolo.monti@uniroma1.it

The influence of large-scale flows on the strength and direction of local winds has been the subject of many studies (e.g. Leuzzi and Monti 1997; Monti and Leuzzi 2005; Petenko *et al.* 2011) that provided insights into the observed flow dynamics. Furthermore, geographic features such as water bodies can modify the slope winds intensity due to changes in roughness, shoreline curvature and source-sink of heat and humidity (Giovannini *et al.* 2015). The presence of urban areas may alter slope winds too (Pelliccioni *et al.* 2016), particularly in narrow valleys (Giovannini *et al.* 2014).

A second important type of mountain wind is the so-called terrain-forced wind, which is produced when a strong large-scale flow combines with local mountain topography giving rise to intense winds with very distinctive local characteristics, such as downslope windstorms like Bora and Föhn. Both the speed and the direction of terrain-forced winds depend on the terrain characteristics such as length and height of the mountain ridges. They generally exceed  $20\text{ ms}^{-1}$  (sometimes  $50\text{ ms}^{-1}$  or even more, see for example Klemp and Durran 1987; Lepri *et al.* 2014) and are caused by intense surface pressure gradients (Whiteman 2000).

The purpose of this study is to determine the main characteristics and peculiarities of the mountain winds typically occurring in Valle Camonica, Italy, which is a wide valley surrounded by elevated mountains (up to 3500 m above the sea level, hereinafter a.s.l.) located in the subrange of the Alps. This makes Valle Camonica representative of a large number of valley-floor slopes in mountainous-type areas. The present analysis, therefore, can be also of great advantage for positioning and management of wind turbines, both for the selection of optimal sites and for the forecast of extreme wind conditions, which can lead to very large turbine loads and potential breakdowns. In perspective, a better characterization of these winds will also be beneficial for the design of large structures that can be challenged by extreme wind gusts that occasionally affect the investigated area. Another important aspect is that Valle Camonica includes Lake Iseo ( $\sim 185\text{ m a.s.l.}$ ), a large subalpine lake that it is expected to produce significant effects on the wind circulation. We note in passing that a more detailed characterization of mountain winds is of great importance also in the field of physical limnology, because the spatial and temporal distribution of the wind stress plays a fundamental role in lake dynamics, as shown for example with reference to the internal waves of lake Iseo (Valerio *et al.* 2012).

In light of the aforementioned issues, two periods are examined in order to investigate typical scenarios occurring during the summer in Valle Camonica. The first one corresponds to a case of high-pressure conditions, when thermally induced winds generated by diurnal heating of the mountains generally prevail over large-scale winds. The second one refers to an event of strong downslope wind, which occurs occasionally in the valley. Even though downslope windstorms take place mostly in winter, they have been sometimes detected also in summer in correspondence of the passage of cold fronts throughout the Alps.

The meteorological model WRF (Skamarock *et al.* 2008) is used to simulate numerically the meteorological field in the valley, while observations collected in a meteorological station located on the lake are used to test the model performance. At present, on the lake surface a meteorological station (Lake Diagnostic System, LDS in the following) is moored at a location where the lake is deeper than 220 m. LDS provides exceptional real-time data that are less influenced than on-shore stations by the local small-scale details of the surrounding topography.

## 2. Area of study, design days for simulations and numerical setup

Lake Iseo is located in the subalpine area of east-central Lombardy at the southern end of Valle Camonica (Fig. 1b and 2). On the south, the valley is open to plain, while high mountains and lateral

valleys are present on both the eastern and western sides. The lake covers a surface area of about 61 km<sup>2</sup> and has a large, mountainous island (Monte Isola, nearly 4.5 km<sup>2</sup>), with a peak elevation of 415 m above the lake surface. That island is located in the middle of the basin, imparting an annulus-like shape to the lake. The wind field over the lake is influenced mainly by the surrounding topography that generates a variety of thermally and dynamically wind driven systems that deeply affect the internal hydrodynamics of the lake (see Valerio *et al.* 2012).

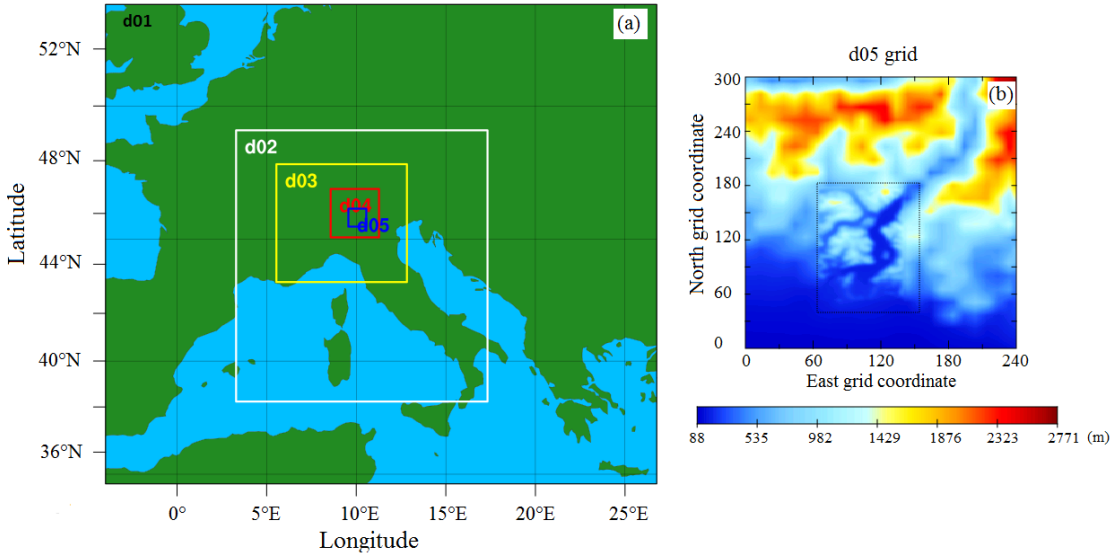


Fig. 1 (a) Domain setup: d01 (resolution 30 km), d02 (10 km), d03 (3.3 km), d04 (1.1 km) and d05 (0.37 km). (b) Topography details of d05 grid (grey scale represents a.s.l. height in meters). The dotted rectangle in the middle corresponds to the area closer to the lake where a refinement of the topography is applied (see text for details).

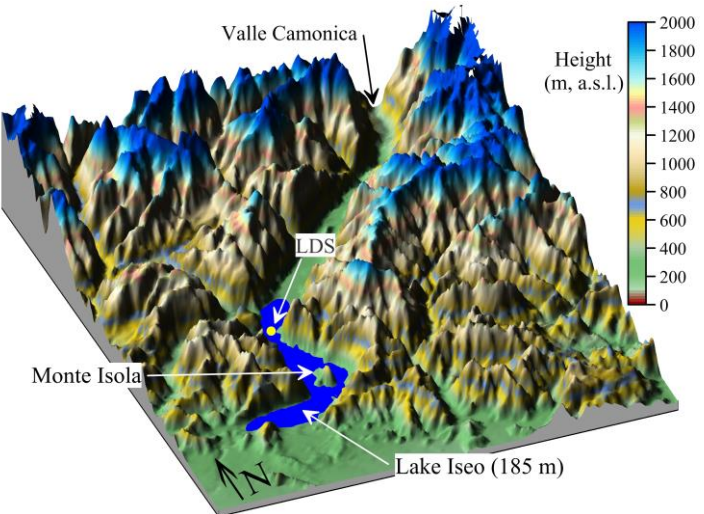


Fig. 2 Sketch of Valle Camonica. The black point indicates the position of LDS.

An example of the meteorological field over Valley Camonica during summer days is shown in Fig. 3, which depicts time histories of wind speed (Fig. 3a) and wind direction (Fig. 3b) collected by LDS station (Fig. 2) from 10 July to 20 July 2010. LDS is a floating station equipped with sensors of wind speed, wind direction and air temperature (see Pilotti *et al.* 2013 for details). The sensors are placed 2 m above the lake surface, in a location that can be considered as free from perturbations due to obstructions. LDS is also equipped with 21 underwater sensors measuring water temperature at 21 depths between 0.25 to 49.75 m. The meteorological data are averaged and stored each 30 s.

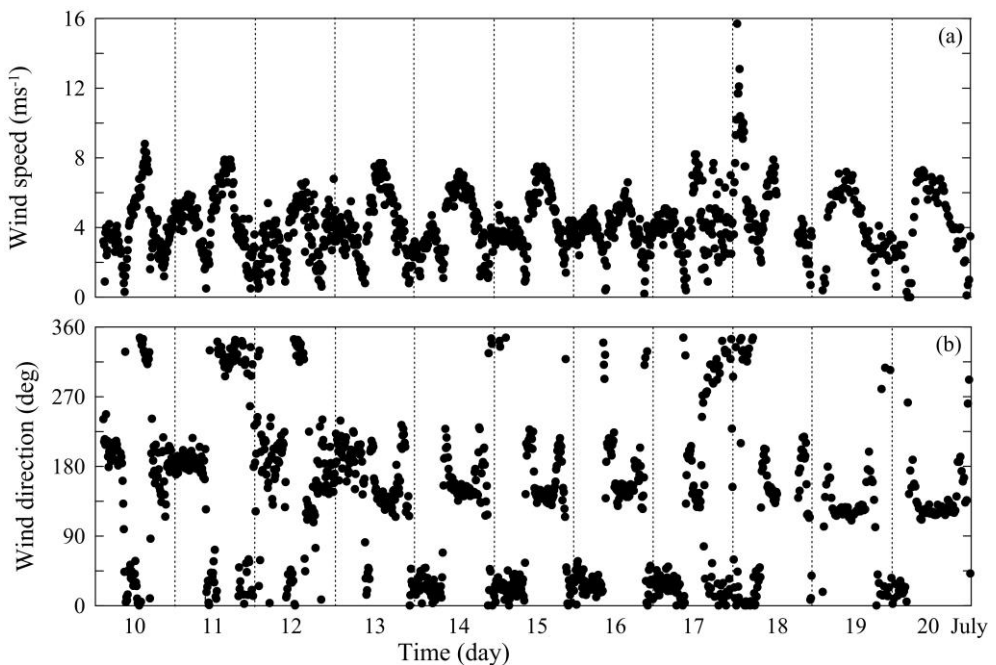


Fig. 3 10-day time histories of (a) wind speed and (b) wind direction measured by LDS at 2 m above the lake surface during the period 10-20 July 2010.  $0^\circ$  indicates winds coming from north,  $90^\circ$  from east. For figure clarity, only 1 data point out of 20 is shown.

It is easy to note from Fig. 3 that a daily periodic behavior is evident in both the wind speed and direction. Due to the valley orientation, both northerly nighttime ( $\sim 315\text{--}45^\circ$ , downslope at LDS) and southerly daytime ( $\sim 135\text{--}225^\circ$ , upslope) winds recur for all the ten days. Both the slope currents show sustained wind speeds, particularly daytime ( $\sim 6\text{--}8 \text{ ms}^{-1}$  at LDS), but the winds subside during morning and evening transitions. Since the flow pattern depicted in Fig. 3 characterizes several months of the year (not shown), it is of interest to estimate the meteorological field in the rest of the valley also for possible applications in energy production (e.g. micro-wind turbines) or pollutant dispersion prediction.

The weather in the period analyzed above is mostly characterized by high-pressure conditions, weak synoptic winds and clear skies. The weather on 18 July, in contrast, is influenced by an eastward propagating cold front, coming from the Atlantic ocean, thereby causing a noticeable cooling trend. The well-defined burst in the wind speed (nearly  $16 \text{ ms}^{-1}$ ) recorded during the night of 18 July is the signature of the passage of the cold front over the Alps. Therefore, as a first step, a numerical simulation is conducted over the period 00 UTC (Universal Time Coordinate) 13 July 2010 to 00

UTC 16 July 2010 in order to analyze in detail the typical daily cycle of the wind speed during high pressure conditions in the whole valley. In a second step, a simulation over the period from 12 UTC 16 July 2010 to 12 UTC 19 July 2010 is carried out to investigate the event of strong wind observed on 18 July. The selection of two cases with distinct synoptic weather conditions is intended to provide an evaluation of the model performance as well as to analyze how synoptic conditions can affect the valley flow.

Regarding the spatial resolution of the grid used in the numerical simulations, we must consider that valley flows generally exhibit complex behaviors and that large variations of sustained winds over a distance of  $\sim$ 100 m in a few minutes are not uncommon. To capture them, microscale ( $<1$  km) weather modeling is essential. Several authors employed WRF for microscale flows modelling; among them Liu *et al.* (2011) used a nested configuration from the synoptic scale to the microscale (sub-km) for wind energy applications. In light of this, the horizontal domain considered for the present numerical simulations consists of five two-way nested grids to cover all spatial scales, from synoptic to local scales (Fig. 1a). In particular, the grids are composed of  $115 \times 100$ ,  $157 \times 169$ ,  $244 \times 220$ ,  $271 \times 271$ ,  $241 \times 301$  cells, with horizontal grid spacing equal to 30, 10, 3.3, 1.1, 0.37 km, respectively. The model employed 35 full Eta levels along the vertical, the lowest computational layer being approximately 8 m above the ground level (a.g.l.) and the top at nearly 21 km a.g.l.. The initial and boundary conditions were supplied by the 6-hourly NCEP Climate Forecast Reanalysis (CFSR) data at  $\sim$ 0.5 degree horizontal resolutions (Saha *et al.* 2010). The innermost domain included Valle Camonica as well as Lake Iseo and its surrounding mountains.

The WRF simulations were performed by using the Noah land surface model (Chen and Dudhia 2001) and the Mellor–Yamada–Janjic Scheme (Janjic 1994) 1.5-order closure turbulent scheme. The microphysics scheme WSM 3-class simple ice scheme (Hong *et al.* 2004) was used in the entire domain, while the Kain–Fritsch (Kain and Fritsch 1993) cumulus scheme was adopted only in the two outer domains. Long-wave and short wave radiations were modeled using the Rapid Radiative Transfer Model (Mlawer *et al.* 1997) and the Dudhia (1989) model, respectively. The effects associated with slopes inclination and topographic shading were taken into account in the radiation schemes.

### 3. Input dataset

With the aim of performing high-resolution simulations, the input data must be carefully chosen in order to provide meaningful information and, at the same time, to avoid any drawback due to numerical instability. The default topography dataset included in WRF has a maximum spatial resolution of 30 arc-seconds ( $\sim$ 1 km at mid-latitude), which does not allow the finest interaction between mountain and local circulation to be captured. For this reason, the topography data SRTM 90 (Shuttle Radar Topography Mission) with a resolution of 3-arc seconds (approximately 90 m at the equator), was adopted for the simulations.

Following indications reported by Giovannini *et al.* (2014), we initially applied to the original dataset a 1-2-1 smooth pass filter to prevent numerical instability at steepest slopes. However, even this procedure made not possible to prevent the crash of simulations due to numerical instability. Having located the causes of instability at the steepest slopes of the northern portion of the grid d05, it was at first used the 30 arc-seconds resolution for the entire d05 grid. Thereafter, it was nested in the area surrounding the lake (see rectangle in Fig. 1b) a portion of the finest topography derived from SRTM 90 and smoothed using the aforementioned filter. In a similar way, but without resorting to the nesting procedure, the WRF default land use 30 arc-seconds USGS dataset was replaced with

the Corine Land Cover (CLC) dataset updated to 2006, provided by the European Environmental Agency (<http://www.eea.europa.eu>). The CLC has a spatial resolution of 100 m and includes 44 classes of different land use categories. The CLC classes were reclassified into the 24 USGS classes, in order to fit the WRF look-up tables. A comparison between the land use map of the inner domain obtained by using the CLC and the original WRF LU dataset is shown in Fig. 4.

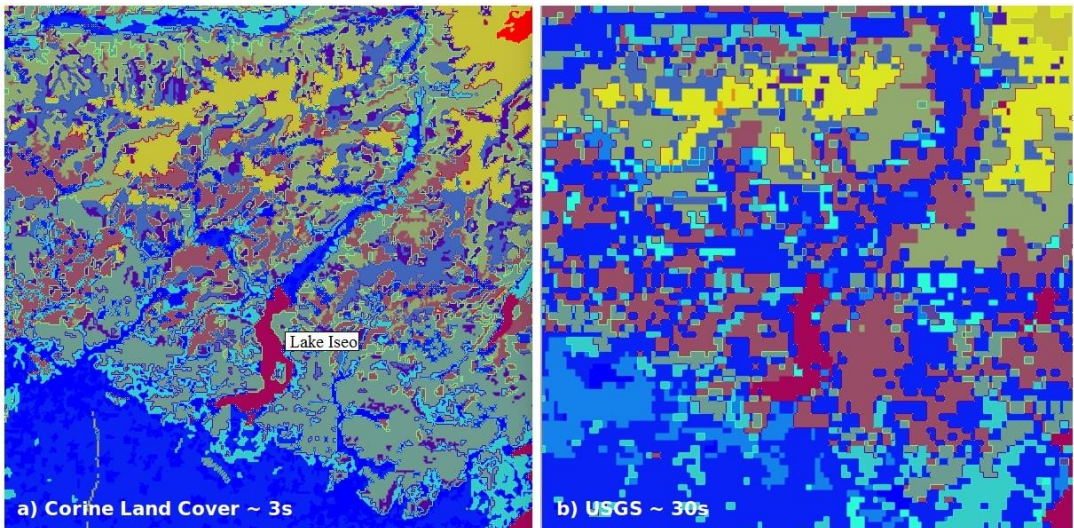


Fig. 4 (a) Map of the 24 land use categories calculated by CLC (~3 sec) dataset for the inner domain. (b) As in (a), but for the original WRF USGS (~30 sec) dataset.

## 4. Results

### 4.1 Analysis of the thermally-induced daily cycle

The first simulation starts at 00 UTC of 13 July 2010 and lasts 72 hours. According to the recommendation of Kleczek *et al.* (2014), we adopted a 22 hours spin-up time. As mentioned in Sect. 2, a high-pressure field was present during those days above North Italy and synoptic winds driven by large-scale pressure gradients were low. Two different runs are performed. In the first one (hereinafter run WRF R1), the temperature of the lake surface is calculated by WRF based on its own original dataset. In order to improve the model performance, in the second run (WFR R2) the lake temperature measured by LDS at a depth of 0.25 m during the two days of simulation is given as input to WRF. The model output on the finest grid are stored every 10 min.

The vector maps depicted in Fig. 5a and 5b show examples of WRF R1 hindcasts of wind speed (at 10 m a.g.l.) and temperature (at 2 m a.g.l.) in the finest grid at 12 LST (Local Standard Time, UTC+1) 14 July and 00 LST 15 July, respectively. In the 12 LST wind hindcast, upslope currents were established in the whole domain and particularly over Valle Camonica (the red tongue feature characterized by high temperatures present in the upper-right portion of Fig. 5a), the latter area showing significant wind speeds, with maximum values of  $\sim 8 \text{ ms}^{-1}$ . It is worth noting that these winds extend also in the plain south to the valley (Pianura Padana), indicating that a well-developed upslope circulation is established. At 00 LST, downslope currents characterize the wind circulation. Compared with the daytime flow pattern, the nocturnal one is much more complex in that isolated

currents flow down from the mountain slopes. Note the lower speed of the downslope winds compared to their upslope counterpart.

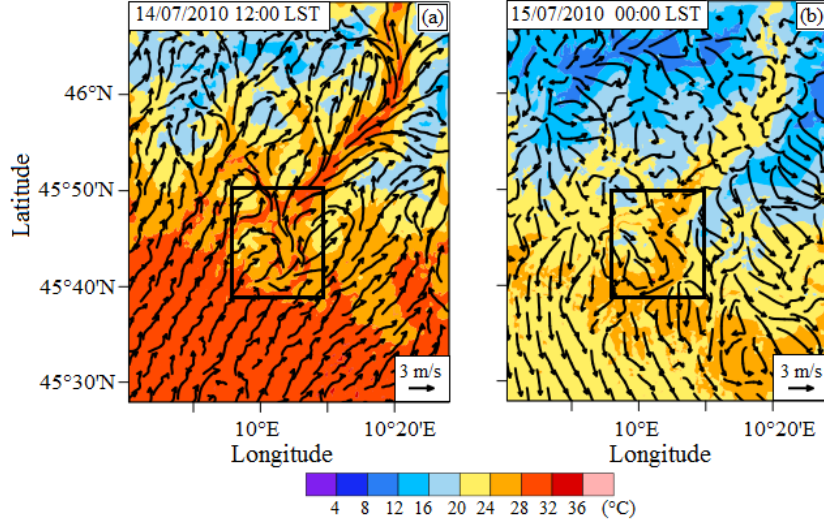


Fig. 5 (a) Wind speed field (finest grid) at 10 m a.g.l. calculated by WRF R1 at 12 LST 14 July. (b) as in (a), but at 00 LST 15 July. The colour scale represents air temperature at 2 m a.g.l.

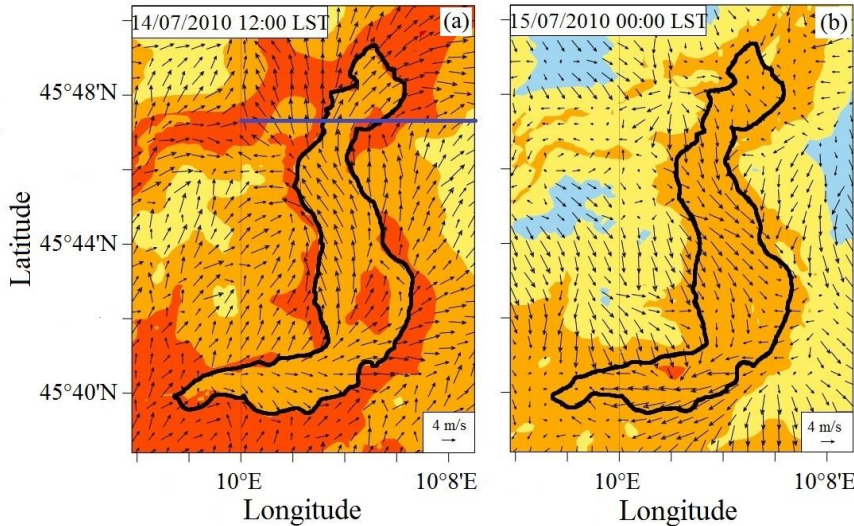


Fig. 6 As in Fig. 5, but here the areas corresponding to the black rectangles drawn in Fig. 5 have been zoomed in.

All the aforementioned features are better represented in Fig. 6, where enlargements of the areas corresponding to the black rectangles drawn in both panels of Fig. 5 are shown. It is evident the flow channeling over Lake Iseo and along the entire Valle Camonica, where the wind is directed upslope (towards north) daytime and reaches a maximum speed of  $\sim 7 \text{ ms}^{-1}$ . Nighttime, the wind is lower ( $\sim 4 \text{ ms}^{-1}$ ) and comes from north and from all the slopes encircling the valley. It is also well evident, particularly at night, the flow separation in correspondence of Monte Isola.

To evaluate the performance of the two model runs, Fig. 7 shows comparisons between simulated (colors) and observed (LDS, black open circles) time histories of wind speed, wind direction and air temperature (Figs. 7a-c, respectively). Since the thermometer and the anemometer installed on LDS were located at 2 m above the lake surface, for ease of comparison the values of the simulated temperature and wind velocity depicted in the figure have been determined by extrapolating the corresponding vertical profiles to 2 m above the lake surface according to the Monin-Obukhov similarity theory (Stull 1988). However, given the position of LDS as well as the small width of the lake and the horizontal grid spacing (370 m), the comparisons must be considered with a degree of caution.

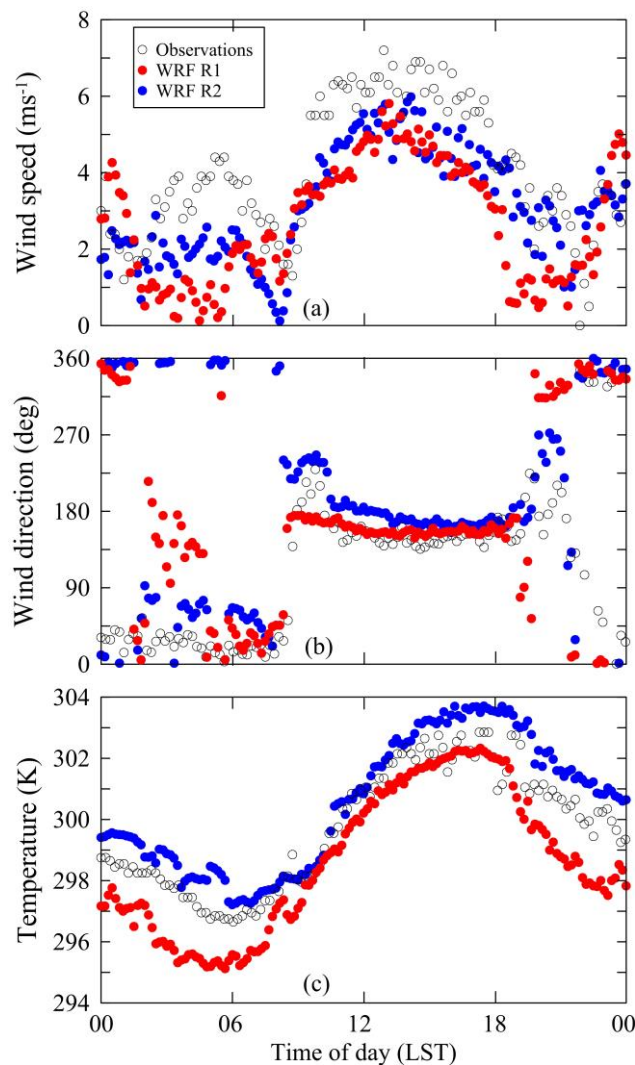


Fig. 7 Comparisons between simulated (red and blue circles) and measured (black open circles) (a) wind speed, (b) wind direction and (c) air temperature on 14 July 2010. All data refer to 2 m above the lake surface. For figure clarity, only 1 data point out of 20 is shown for the observed data set.

Overall, the agreement is reasonably good for WRF R2 (blue circles), while WRF R1 (red circles)

shows nighttime a severe underestimation of both temperature and wind speed. Therefore, the lake temperature seems to be an important parameter to correctly simulate the meteorological field over the lake surface (and therefore in the valley), particularly at night. The simulated time of occurrence of the transition between upslope and downslope wind (and *vice versa*) agrees well with the observed one. The wind, coming from south-southwest (i.e. aligned with Valle Camonica) during the daytime, suddenly reverses, flowing down slope from north-northeast at night. It is worthwhile noticing the discontinuous pattern of the air temperature (Fig. 7c) simulated nighttime (less evident in the observations), which might be a signature of the passage of different downslope currents coming from separate peaks of the mountain range encircling the valley. These currents combine to form a single drainage wind that flows down the valley floor towards the valley outlet.

Information on the vertical structure of the flow can be obtained from Fig 8, where plane-view pictures of the wind speed simulated by WRF R2 along a vertical plane passing for LDS (see Fig. 6) are shown. The figure highlights the differences existing between the nighttime flow pattern (Fig. 8a) and the daytime one (Fig. 8b). In the latter case, in particular, it is well evident the air layer corresponding to the upslope wind, which thickness is  $\sim 600$  m. Winds of order  $7 \text{ ms}^{-1}$  are present also at elevated levels ( $\sim 500$  m above the lake surface), in consonance with what is usually found in mountainous sites during daytime. As the figure reveals, the katabatic flow seems to be not well structured along the vertical and does not show the clear low-level maximum generally observed in drainage winds (see for example Monti *et al.* 2014). This fact is probably related to the vertical spatial resolution adopted near the surface to build the numerical grid, not fine enough to resolve all the details of the drainage flow at low levels. Near the wind-speed maximum, in fact, the turbulence can be highly anisotropic and a very fine grid is necessary to properly simulate the flow field (see for example Cuxart and Jiménez 2007).

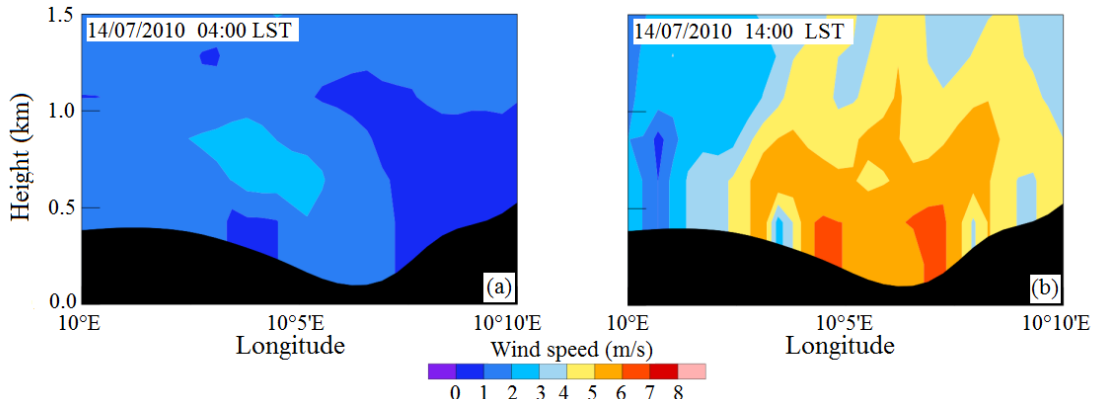


Fig. 8 (a) Maps of the wind speed simulated by WRF R2 at 04 LST of 14 July along the vertical plane passing for LDS. (b) As in (a), but at 14 LST.

#### 4.2 Analysis of the event of strong katabatic wind

The second case chosen for the analysis is the event of strong katabatic wind that occurred the night of 17-18 July, when a cold front heading east passed throughout the Alps, causing a sudden decrease of both air temperature and pressure over the Valle Camonica and the Alps. The numerical simulation starts at 12 UTC 16 July 2010 and lasts 72 hours. Hereinafter, the results refer only to WRF R2.

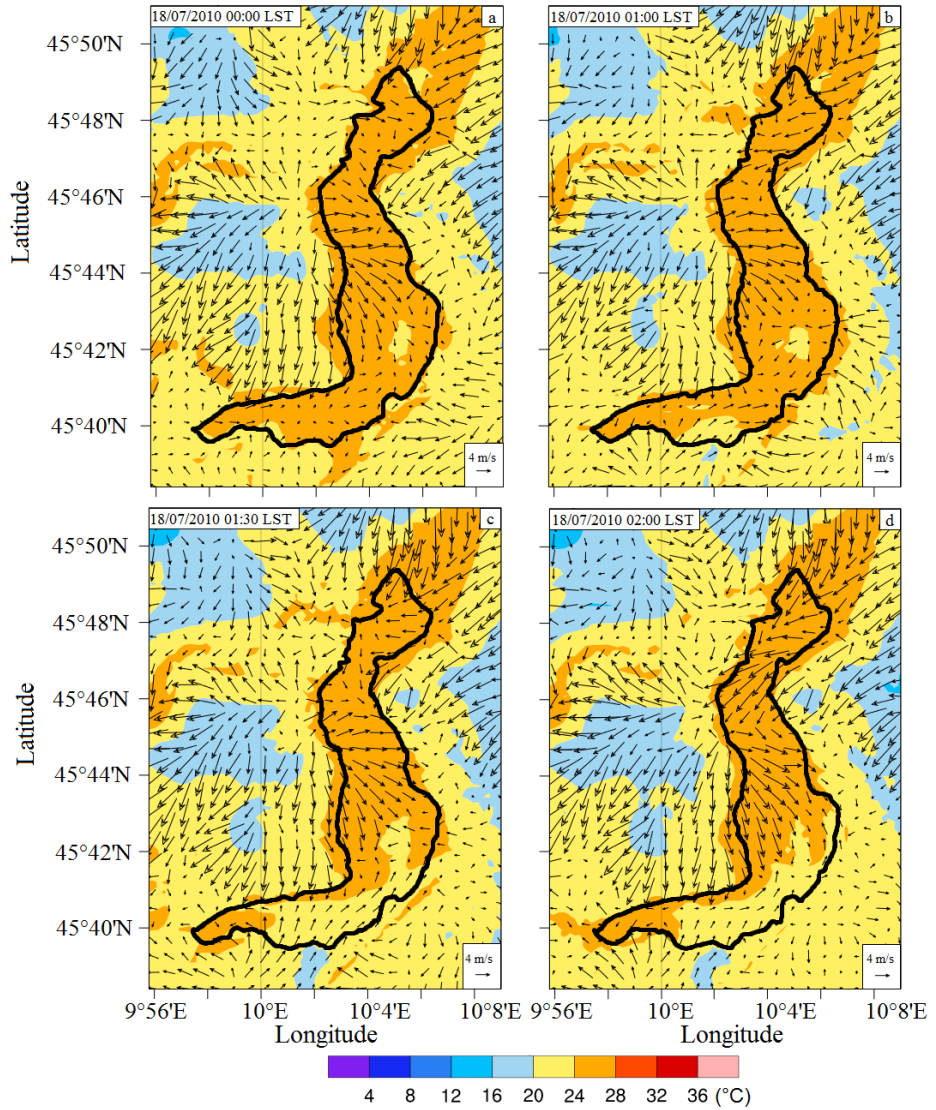


Fig. 9 Wind speed fields at 10 m a.g.l. simulated by WRF R2 for different hours of 18 July in the area surrounding the lake. Colors represent air temperature simulated at 2 m a.g.l.

Figure 9 shows the velocity and temperature fields simulated at different hours of the night of 18 July, while the time histories of wind speed, wind direction and turbulent kinetic energy ( $q$ ) simulated at four heights belonging to the vertical profile passing for LDS are shown in Fig. 10 (lines). While daytime the observed wind speeds (Fig. 10a) are comparable to those observed on 14 July (see Fig. 7a), nighttime they are nearly a factor of three higher, reaching maxima of order  $16 \text{ ms}^{-1}$ . As the panels depicted in Fig. 9 reveal, the sudden increase in wind velocity at 23 LST 17 July is caused by an intense downslope current moving from north down the valley.

Overall, the modeled wind speed and direction match the measured data, even though the wind speed is underestimated nighttime by about 40%, and the simulated transition between downslope

and upslope wind occurs nearly 2 hours later than the observed one. Note that, during the night, both wind speed and direction do not change appreciably along the vertical direction.

During the period of strong winds, the flow is accompanied by large turbulent kinetic energy, particularly near the surface, where a peak of  $\sim 5 \text{ m}^2\text{s}^{-2}$  at 10 m a.g.l. occurs at about 00 LST 18 July. It is noticeable that the area interested by strong winds covers only the north-central portion of the lake, while in the southern part of it the wind is lower and comes from south-southwest.

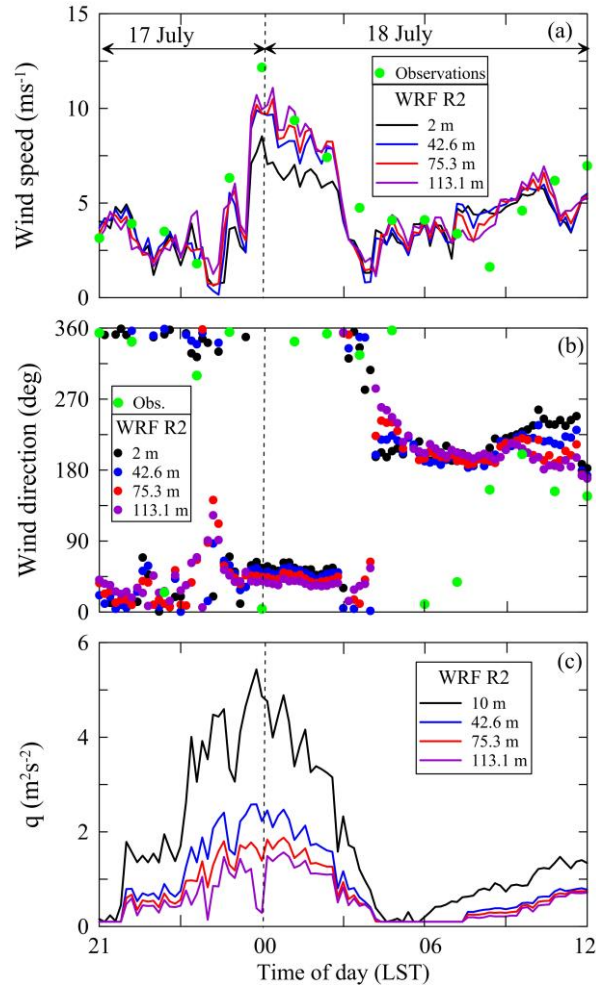


Fig. 10 Time histories of the simulated (a) wind speed, (b) wind direction and (c) turbulent kinetic energy,  $q$ , during 17-18 July 2010 at several heights above the ground level along the vertical profile passing for LDS. The green circles in (a) and (b) refer to data observed at  $z=2 \text{ m}$  a.g.l. at LDS (for figure clarity, only 1 data point out of 12 is shown).

This flow pattern had held for the whole night, followed by a daytime flow similar to that observed the 14 July. The different nature of this nocturnal event with respect to that observed the night of 14 July can be also deduced by comparing the vertical structure of the flow simulated at 02 LST of 18 July (see the wind-speed map in Fig. 11) with that reported in Fig. 8a.

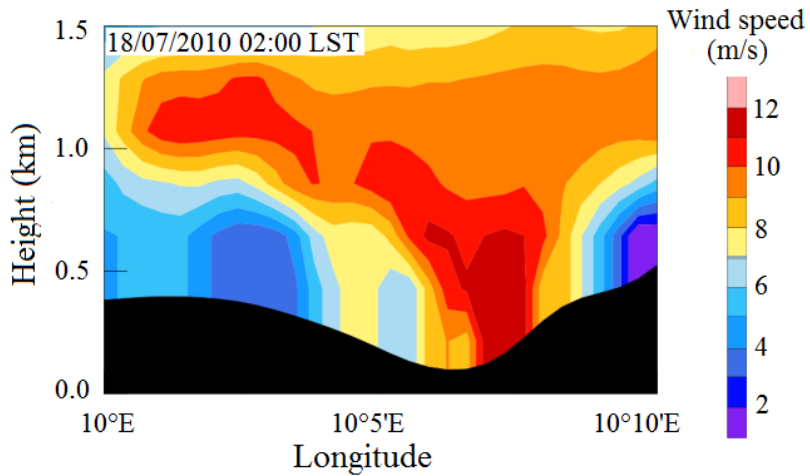


Fig. 11 As in Fig. 8, but for the wind speed simulated at 02 LST of 18 July

For the present case, in fact, the downslope flow occupies the whole vertical section of the valley and the elevated layers as well. Regions of low wind speed along the valley slopes are also evident, which can be attributed to local topographic characteristics of the terrain.

## 5. Summary and Conclusions

This study investigated the wind circulation in an alpine valley (Valle Camonica, Italy), characterized by the presence of a large subalpine lake (Lake Iseo). The meteorological model WRF was used to simulate the thermally-induced local circulation that typically occurs summertime in the valley. Given the complex topography of the area, to properly account for the finest interaction between mountains and local circulations, the topography taken by SRTM 90 (Shuttle Radar Topography Mission, resolution of approximately 90 m) was used in place of the default topography dataset included in WRF (maximum spatial resolution of  $\sim 1$  km at mid-latitude).

The results show that the whole valley was characterized by the typical upslope and downslope winds regime caused by diurnal variation of the terrain temperature. Comparisons with observational data taken above the lake surface suggest that the lake temperature has a noticeable influence on the air temperature and the wind field in the valley, particularly at night. Its knowledge, therefore, can be important in alpine micrometeorological simulations. An additional simulation was performed to investigate the wind field during the passage of a cold front over the Alps, which induced strong downslope currents coming from the upper part of the valley.

By contributing to a better comprehension of the wind regime in the pre-alpine lakes region, this study leads to an improved evaluation of the wind potential of this area. From a methodological point of view, it also suggests how numerical modeling can be used to locate the most interesting spots for wind exploitation.

## Acknowledgments

We thank Prof. Jörg Imberger and all his research team for their contribution to the acquisition of the field data used in this paper.

## References

- Chen, F. and Dudhia, J. (2001), “Coupling an advances land surface-hydrology model with the Penn State-NCAR MM5 modeling system. Part I: model implementation and sensitivity”, *Mon. Weather Rev.*, **129**, 569–585.
- Cuxart, J. and Jimenez, M.A. (2007), “Mixing Processes in a Nocturnal Low-Level Jet: An LES Study”, *J. Atmos. Sci.*, **64**, 1666-1679.
- Dudhia, J. (1989), “Numerical study of convection observed during the Winter Monsoon Experiment using a mesoscale two-dimensional model”, *J. Atmos. Sci.*, **46**, 3077–3107.
- Fernando, H.J.S., Lee, S.-M., Anderson, J., Princevac, M., Pardyjak, E.R. and Grossman-Clarke, S. (2001), “Urban Fluid Mechanics: air circulation and contaminant dispersion in cities”, *Environ. Fluid Mech.*, **1**, 107-164.
- Giovannini, L., Laiti, L., Zardi, D. and de Franceschi, M. (2015), “Climatological characteristics of the Ora del Garda wind in the Alps”, *Int. J. Climatol.*, **35**(14), 4103-4115.
- Giovannini, L., Zardi, D., de Franceschi, M. and Chen, F. (2014), “Numerical simulations of boundary-layer processes and urban-induced alterations in an Alpine valley”, *Int. J. Climatol.*, **34**, 1111–1131.
- Hong S.-Y., Dudhia J. and Chen, S.-H. (2004), “A revised approach to ice microphysical processes for the bulk parameterization of clouds and precipitation”, *Mon. Weather Rev.*, **132**, 103–120.
- Janjic, Z.I. (1994), “The Step–Mountain Eta Coordinate Model: Further developments of the convection, viscous sublayer, and turbulence closure schemes”, *Mon. Weather Rev.*, **122**, 927–945.
- Kain, J.S. and Fritsch, J.M. (1993), “Convective parameterization for mesoscale models: the Kain–Fritsch scheme”, *The Representation of Cumulus Convection in Numerical Models*, Emanuel K.A., Raymond D.J. (eds.). American Meteorological Society, Boston, MA, USA.
- Kleczeck, M.A., Steeneveld, G.J. and Holtslag, A.A. (2014), “Evaluation of the weather research and forecasting mesoscale model for GABLS3: impact of boundary-layer schemes, boundary conditions and spin-up”, *Bound.-Layer Meteorol.*, **152**(2), 213-243.
- Klemp, J.B. and Durran, D.R. (1987), “Numerical modelling of Bora winds”, *Meteorol. Atmos. Phys.*, **36**(1-4), 215-227.
- Lepri, P., Kozmar, H., Večenaj, Ž, and Grisogono, B. (2014), “A summertime near-ground velocity profile of the Bora wind”, *Wind Struct.*, **19**(5), 505-522.
- Leuzzi, G., and Monti, P. (1997) “Breeze Analysis by Mast and Sodar Measurements”, *Nuovo Cimento C*, **20**, 343-359.
- Liu, Y., Warner, T., Liu, Y., Vincent, C., Wu, W., Mahoney, B. and Boehnert, J. (2011), “Simultaneous nested modeling from the synoptic scale to the LES scale for wind energy applications”, *J. Wind Eng. Ind. Aerodyn.*, **99**(4), 308-319.
- Mlawer, E.J., Taubman, S.J., Brown, P.D., Iacono, M.J. and Clough, S.A. (1997), “Radiative transfer for inhomogeneous atmospheres: RRTM, a validated correlated-k model for the longwave”, *J. Geophys. Res.*, **102**(D14), 16663–16682.
- Monti, P., Fernando, H.J.S. and Princevac, M. (2014), “Waves and turbulence in katabatic winds”, *Environ. Fluid. Mech.*, **14**, 431-450.
- Monti, P. and Leuzzi, G. (2005), “A numerical study of mesoscale airflow and dispersion over coastal complex terrain”, *Int. J. Environ. Pollution*, **25**, Nos. 1/2/3/4, 239-250.
- Pelliccioni, A., Monti, P. and Leuzzi, G. (2016), “Wind-speed profile and roughness sublayer depth modelling in urban boundary layers”, *Boundary-Layer Meteorol.*, **160**, 225-248.
- Petenko, I., Mastrantonio, G., Viola, A., Argentini, S., Coniglio, L., Monti, P. and Leuzzi, G. (2011), “Local circulation diurnal patterns and their relationship with large-scale flows in a coastal area of the Tyrrhenian Sea”, *Bound.-Layer Meteorol.*, **139**, 353-366.
- Pilotti, M., Valerio, G., Leoni, B. (2013), “Data set for hydrodynamic lake model calibration: a deep pre-alpine case”, *Water Resour. Res.*, **49**, 1–5, doi:10.1002/wrcr.20506.
- Saha, S., et al. (2010), NCEP Climate Forecast System Reanalysis (CFSR) 6-hourly Products, January 1979

to December 2010, <http://dx.doi.org/10.5065/D69K487J>, Research Data Archive at the National Center for Atmospheric Research, Computational and Information Systems Laboratory, Boulder, Colo. Accessed 01 Oct 2015.

Skamarock, W.C., Klemp, J.B., Dudhia, J., Gill, D.O., Barker, D.M., Duda, M.G., Huang, X.-Y., Wang, W. and Powers, J.G. (2008), "A description of the advanced research WRF version 3", Technical Note TN-475+STR, NCAR, USA.

Stull, R.B. (1988), *An Introduction to Boundary-Layer Meteorology*, Kluwer Academic Publishers, Dordrecht, The Netherland.

Valerio, G., Pilotti, M., Clelia, L.M. and Imberger, J. (2012), "The structure of basin—scale internal waves in a stratified lake in response to lake bathymetry and wind spatial and temporal distribution: Lake Iseo, Italy", *Limnol. Oceanogr.*, **57**(3), 772-786.

Whiteman, C.D. (2000), *Mountain Meteorology: Fundamental and Applications*, Oxford Univ. Press, New York, NY, USA.